Journal of Cleaner Production 180 (2018) 34–42

Contents lists available at ScienceDirect

Journal of Cleaner Production

journal homepage: www.elsevier.com/locate/jclepro

Compositional characteristics of black-carbon and nanoparticles in air-conditioner dust from an inhabitable industrial metropolis☆

Muhammad Ubaid Ali [a, b], Guijian Liu [a, b, *], Balal Yousaf [a, b], Qumber Abbas [a], Habib Ullah [a], Mehr Ahmad Mujtaba Munir [a], Hong Zhang [a]

[a] CAS-Key Laboratory of Crust-Mantle Materials and the Environments, School of Earth and Space Sciences, University of Science and Technology of China, Hefei, 230026, China

[b] State Key Laboratory of Loess and Quaternary Geology, Institute of Earth Environment, The Chinese Academy of Sciences, Xi'an, Shaanxi, 710075, China

ARTICLE INFO

Article history:
Received 3 August 2017
Received in revised form
2 January 2018
Accepted 19 January 2018
Available online 28 January 2018

Keywords:
Black carbon
Nanoparticle composition
Air conditioner dust
Metropolitan

ABSTRACT

Atmospheric dust, especially air-conditioner dust in urban-industrial environments, can act as a significant sink for both black carbon and nanoparticles posing allied health risks to the air conditioner repairman as well as to local inhabitants. However, the chemical composition of black carbon/nanoparticles in air-conditioner dust and their association with potentially toxic elements remain uncertain. The present study investigate the black carbon and nanoparticles compositions of air-conditioner dust and their associated potentially toxic elements, as an indicator of indoor air-pollution. The black carbon and nanoparticles in air-conditioner dust, were comprehensively characterized using array-based techniques including Inductively Coupled Plasma-Mass Spectrometry, particle size distribution, Scanning Electron Microscopy, Transmission electron microscopy along with Energy-dispersive X-ray spectroscopy and selected area-(electron) diffraction, from metropolitan area of Hefei, China. Geo-accumulation index values of air-conditioner dust reveal Lead, Tin, Arsenic and Cadmium are under Geo-accumulation Classes V-VI level of contamination. The majority of the particles were found to be in the ultrafine nanoparticles range (<100 nm). A strong correlation was found between black carbon and total potential toxic elements content ($R^2 = 0.79$). The metallic nanoparticles (Iron, Copper and Lead) and black carbon were identified using Scanning Electron Microscopy/Transmission electron microscopy along with Energy-dispersive X-ray spectroscopy/selected area (electron) diffraction mode. Using array-based techniques seems to be a useful tool to study the black carbon and nanoparticles in air-conditioner dust. It is the first demonstration presenting evidence for the concept of air-conditioner dust as a sink for black carbon/nanoparticles bound potentially toxic elements in the urban-industrial environments, as an ultimate source of environmental pollutants.

1. Introduction

Air conditioning (AC) system is used worldwide to provide thermal comport as well as a healthy air quality in the indoor environment (Yu et al., 2009). The indoor air quality is deteriorated by a variety of factors including temperature, air circulation, humidity, particulate matter (PM) pollution, biological and gaseous pollutant (Graudenz et al., 2005). The origin of indoor particulate can be divided into two categories that are indoor and outdoor pollution sources. Particles released by indoor sources like smoking, cooking, heating, cooling, construction, furnishing and burning are mostly ultrafine which constitute 80% in terms of particle count (See et al., 2006). Particles released from the outdoor environment penetrate through doors, ventilation system, windows and AC filters for fresh air (Gramotnev and Ristovski, 2004). The air loaded with PM is filtered by AC in order to improve the indoor air quality

☆ Muhammad Ubaid Ali and Balal Yousaf contributed this work equally and should be considered as a co-first author.

* Corresponding author. CAS-Key Laboratory of Crust-Mantle Materials and the Environments, School of Earth and Space Sciences, University of Science and Technology of China, Hefei, 230026, China.

E-mail addresses: ubaid@mail.ustc.edu.cn (M.U. Ali), lgj@ustc.edu.cn (G. Liu), balal@ustc.edu.cn (B. Yousaf), qumber@mail.ustc.edu.cn (Q. Abbas), Habib901@mail.ustc.edu.cn (H. Ullah), muju212@mail.ustc.edu.cn (M.A.M. Munir), Zhang121@mail.ustc.edu.cn (H. Zhang).

https://doi.org/10.1016/j.jclepro.2018.01.161
0959-6526/

which is widely used and economical method (Yu et al., 2009). Filters are the most important part of AC and it has been investigated that these filters can remove pollutants efficiently in a steady manner which get deposited on these filters (Bekö et al., 2006). Irrespective of the fact that air filtration by AC filters improve the air quality these filter can be a source of contamination as a lot of nanoparticles (NPs) along with organic and inorganic pollutants including organic carbon, trace elements, nitrate, sulfate and volatile organic compounds get deposited on these filters of AC (Verdenelli et al., 2003).

NPs having a diameter of 0.1 μm or less are of key importance because these can remain suspended in the air for a long time as compared to other coarse size PM and can be transported for a long distance (Yinon et al., 2010). One of the basic property of NPs is its large surface area to volume ratio which makes it capable of adsorbing a large amount of potential toxic elements (PTEs) and it is the most dominant particulate in the atmosphere (Lighty et al., 2000). A variety of sources contribute as a source of PTEs and black carbon (BC) NPs including outdoor and indoor activities (Isaxon et al., 2015; Wan et al., 2011). Elevated concentration of chromium (Cr), zinc (Zn), copper (Cu), manganese (Mn), lead (Pb) and cadmium (Cd) NPs are attributed to cigarette smoke, use of cosmetics, construction and demolition (Dundar and Altundag, 2002), paints, carpet materials and also vehicular emission in form of fine dust (Chen et al., 2010), while in indoor environment use of gasoline and lead containing paints play their role in Pb emission (Olujimi et al., 2015). Nickel (Ni) and iron (Fe) NPs originates as a result of coal combustion, fossil fuel (Ullah et al., 2017), waste products incineration, automobile emissions, decay of old engine, smelting process, and industries in outdoor environment while in indoor environment it mainly released from smoking, use of stainless steel utensils and low category jewelry (Cempel and Nikel, 2006). Use of lubricating oil (Patel et al., 2012) and fossil fuel increase the concentration of Aluminum (Al), Mn, magnesium (Mg) and Fe-NPs and other PTEs (Yousaf et al., 2017). Another NPs quite important due to its high magnitude toxicity and ultrafine size is soot (BC or elemental carbon) (Hussein et al., 2006). BC is released as result of incomplete combustion by a variety of sources including indoor and outdoor sources and weathering of graphite carbon in rocks (Zhang et al., 2015). The two main form of BC are char and soot, char is produced at low temperature than soot with a size range of 1–100 μm that is larger than soot (Zhan et al., 2016). Other than this it can be found in NPs form with a size range of <100 nm that is mostly released is a major part of diesel. Temperature is the key factor deciding the size and form of BC (Sahu et al., 2014). BC is of special importance because of its long range transport, climate change role and due to its large surface area it is involved in a variety of heterogeneous activates (Johnson et al., 2005). Large surface to volume ratio and large number of nanopores of BC-NPs are the main reason for its high sorption and its relation with other PTEs which are produced along with BC during combustion process (Glaser et al., 2005). Previous studies revealed that PTEs concentration (Niu et al., 2010), and BC concentration increase with a decrease in particle size (Gramsch et al., 2014). NPs are a potential health hazard due to its small size it can penetrate deep into the respiratory track and cause severe health problems (Ali et al., 2017b).

Up till now no detailed study has been conducted focusing the compositional and Nano characteristics of dust accumulated on AC filters. The current study aim to investigate the following objectives: (1) To evaluate the concentration and pollution characteristics of PTEs in AC dust collected from metropolitan area of Hefei, China (2) To comprehensively characterize BC and dominant NPs in AC dust using array-based techniques including Inductively Coupled Plasma-Mass Spectrometry (ICP-MS), aerosolization and Scanning Electron Microscopy (SEM)/Transmission electron microscopy (TEM) along with Energy-dispersive X-ray spectroscopy (EDS)/selected area (electron) diffraction mode (SAED) (3) To find out relation between BC and ΣPTEs in AC dust in an urban environment.

2. Materials and methods

2.1. Site description and sample collection

The present study was conducted in Hefei capital of Anhui province with an area of 11,408 km^2 and population 4.6 million lying in upper limits of Yangtze delta. It is situated at 117° 11 to 117° 22 east longitude and 32° 48 to 31° 58 north latitude lies within the north subtropical climate zone. It is a prefecture level city of Hefei administrators with 9 county-level division including 4 districts namely Yaohi, Luyang, Shushan and Baohe district. In this study, houses were selected randomly from different areas of Hefei and the AC filters (split AC 1.5–3 tons) from selected locations were properly cleaned at the end of January in order to remove the preexisting dust and pollutants (Fig. 1). Sampling was done in June, and July because these are the hottest months with prevailing dry condition and the use of air conductions is at its peaks in these months. In this investigation, 71 samples were collected using a plastic brush, paper sheets and air tight polythene bags. To ensure proper collection of samples the dust from filters were collected in a closed room and the filters were tapped slowly in order to avoid the interference of air as the dust deposited on these filter was of very minute size that can resuspend with ease. The samples were then transferred to airtight polythene bags. These samples were further sieved at a mesh of 200 (particles size < 75 μm) and were air dried for 48 h in order to carry out further analysis.

2.2. ICP-MS analysis and geo-accumulation index (I_{geo})

AC dust samples were digested in the acid mixture using the method described by Yousaf et al. (2016). Agilent 7500cx Inductively Coupled Plasma Mass Spectrometer (ICP-MS, Agilent Technologies, and Santa Clara, CA, USA) was used to identify trace element concentrations in acid-digested AC dust samples. Instrument calibration is given in supplementary information. A total of 18 trace elements (barium (Ba), lithium (Li), Mg, Cd, tin (Sn), Pb, gallium (Ga), arsenic (As), strontium (Sr), Cu, Ni, Fe, Cr, Mn, vanadium (V), thallium (Ti) and Al) were identified in this study. BC concentration in AC dust sample was identified using thermal-optical reflectance method (TOR) according to Zhan et al. (2016).

To find the accumulation of trace elements, geo-accumulation index (Table 1) was used to find out a single element pollution status in the environment (Müller, 1979).

$$Igeo = log^2\left(\frac{C_{sample}}{1.5 \times C_{background}}\right) \quad (1)$$

Where, l_{geo} is the geo-accumulation index for different trace element. C_{sample} is the concentration of PTEs in sample and $C_{background}$ is the element background value. To avoid variation in background values a constant of 1.5 was added. These background fluctuations are basically due to lithogenic variation in the dust.

2.3. Aerosolization of AC dust

Samples selected on the bases of PTEs concentration and total mass were aerosolized using the dry dispersion (Disperser) method introduced by Tiwari et al. (2013) based on vacuum generator and

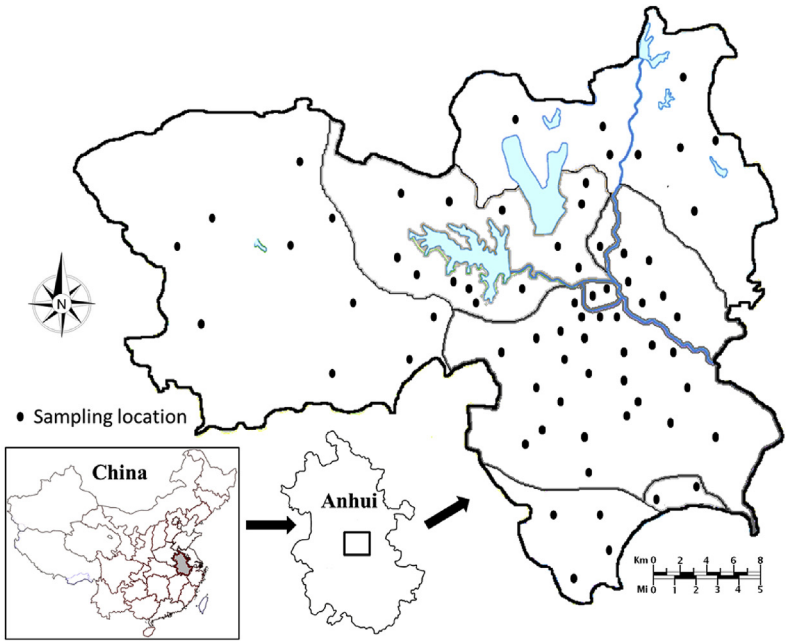

Fig. 1. Map showing sampling locations for Air conditioner dust samples from metropolitan area of Hefei, China.

Table 1
Geo-accumulation classes to identify single element pollution status with respect to dust quality.

I_{geo} value (log_2 (x))	I_{geo} class	Qualitative designation of road dust[a]
$I_{geo} \leq 0$	0	Uncontaminated
$0 < I_{geo} \leq 1$	1	Uncontaminated to moderately contaminated
$1 < I_{geo} \leq 2$	2	Moderately contaminated
$2 < I_{geo} \leq 3$	3	Moderately to heavily contaminated
$3 < I_{geo} \leq 4$	4	Heavily contaminated
$4 < I_{geo} \leq 5$	5	Heavily to extremely contaminated
$I_{geo} > 5$	6	Extremely contaminated

[a] Quantitative classes of road dust and their respective designations given by Müller (1979).

operated at an air flow of 10 L min $^{-1}$ (Yang et al., 2016). To eliminate coarse size particles each sample was passed through (URG-2000-30EN, URG Corp.) PM2.5 cyclone. The remaining sample was then passed through three sampling stages including (1) Teflon filter with 47 mm diameter and a pore size of 0.1 μm (2) particle size sampler loaded with TEM grids (3) Scanning mobility particle sizer (3936NL, TSI) was used to characterize the aerosolized samples with in a size range of 15–650 nm. The method was validated using Titanium dioxide (TiO_2) nanoparticles 7 and 50 nm purchased from MK Impex Corp. (Mississauga, ON, Canada) and TiO_2 20 nm obtained from Nanostructured & Amorphous Materials Inc. (Houston, TX, USA). The powder was basically composed of TiO_2 Anatase which was 95% in case of 7 and 98% in case of 50 nm with an average particle size of 7 and 50 nm, while 99% in case of 20 nm with an average particle size of 10 and 30 nm according to manufactures specification guide. The instruments were tested using TiO_2 material in order to check the accuracy of the method used.

2.4. SEM/TEM analysis

The morphological characteristics of AC dust were determined using scanning SEM (ESEM, FEI Quanta 250 FEG) equipped with EDS. SEM along with EDS is a useful tool to provide metallurgical testing and elemental composition using American Society for Testing and Materials (ASTM) B748 test method. It can provide qualitative and semi-quantitative elemental composition along with along with coating and foreign inorganic substances identification with resolution up to 5× to 30,000×. The results are generated in form of black and white images for proper interpretation. The EDS detector separates the characteristic X-rays of different energy spectrums that's is typically charted with X-ray wavelength versus energy or intensity (KeV) and label each element. In order to identify the elements, the peak values on x-axis were matched with a known wavelength of each element to find out the elemental composition of the sample. In order to provide visual information which was based on contrast difference between levels of different atomic number backscattered electron (BSE) mode was used. An adequate portion of the AC dust sample was sprinkled over a double sided carbon tape and was mounted on scanning electron microscope. The NPs size and composite was determined using TEM along with EDS system (JEM 2100 TEM/Scanning-TEM, JEOL Corporation). For TEM images a drop of Aqueous AC dust solution was placed on a carbon-coated copper grid and was dried in dust free environment. SAED mode was used to record the electron diffraction patterns of crystalline and semi-crystalline phases in selected areas.

2.5. Thermal optical reflectance

The AC dust samples were air dried and sieved in order to remove particles greater than 1 mm size and the remaining sample was grinded using agate motor in order to homogenize the sample. The samples were dried at 40 °C and stored in air tight containers. In order to extract BC, acid free treatment method was used. In order to remove carbonates the sample was treated with HCL, then a mixture of Hydrochloric acid (HCL) and Hydrofluoric acid (HF) was used to remove the silicates and at last again treated with HCL to eliminate the remaining Fluorite and Carbonates. For final analysis, the samples were rinsed and filtered through pre-fired (850 °C, 3 h) quartz filter of 47 mm the BC content was then measured using thermal optical reflectance method using Desert Research Institute (DRI) Model 2001 Carbon Analyzer (Atmoslytic

Inc., Calabasas, CA) following the IMPROVE protocol.

2.6. Quality control and data analysis

Quality control and data precision were insured using certified standard material (GBW07406) obtained from National Center for Standard Material of China (NCMSMC). For all PTEs determined in this study the recovery rate (95.3–103.8%) in standard reference material was within the limit of certified reference material. The recovery range for the digested solution of known PTEs was between 91.14 and 103.6% with the acceptable precision level in a range of ±5 wt %. The calibration curves were linear within the range (R^2 > 0.99) demonstrating the accuracy and consistency of analytical technique for PTEs determination. For descriptive statistics and data analysis PASW Statistics 18 software (SPSS Inc., Chicago, IL, USA). All graphs were plotted using Sigmaplot 11.0 (Systat Software Inc., San Jose. California, USA).

3. Results and discussion

3.1. Potentially toxic elements and pollution characteristics of AC dust

The mean concentration and statistical summary of PTEs (μg g^{-1}) in AC dust samples from the metropolis of Hefei, China are given in Fig. 2 and Table S1, respectively. The ascending order for mean concentration values of elements in AC dust was Cd < As < Sn < V < Ba < Ni < Ga < Pb < Cr < Sr < Li < Cu < Mn < BC < Ti < Zn < Mg < Fe < Al. The mean concentrations of all the trace elements were found to be high as compared to the corresponding background values except for As and Cd with mean values of 3.5 and 0.6 μg g^{-1}. The mean concentration of BC was 126.7 μg g^{-1} with a standard deviation of 39.4 μg g^{-1}. The correlation among elements found in AC dust is demonstrated in supplementary Table. S2 and Fig. S1. Single element pollution status was determined using I_{geo} (geo-accumulation index) which categories the pollution levels into 7-enrichment classes (0–6) based on the severity of contamination. The I_{geo} values of 18 trace elements in AC dust found using Equation (1) are demonstrated in (Fig. 3). The mean I_{geo} value of Al, Ti, V, Cr, Mn, Fe, Ni, Cu, Zn, Ga, As, Sr, Sn, Pb, Tl, Li, Mg and Ba in AC dust were −1.68, 3.28, −1.65, −1.49, −2.43, −1.06, −0.88, 2.06, 2.71, 0.09, 4.98, 0.71, 4.05, 7.76, 8.63, −5.22, −1.45, −3.76. In the case of

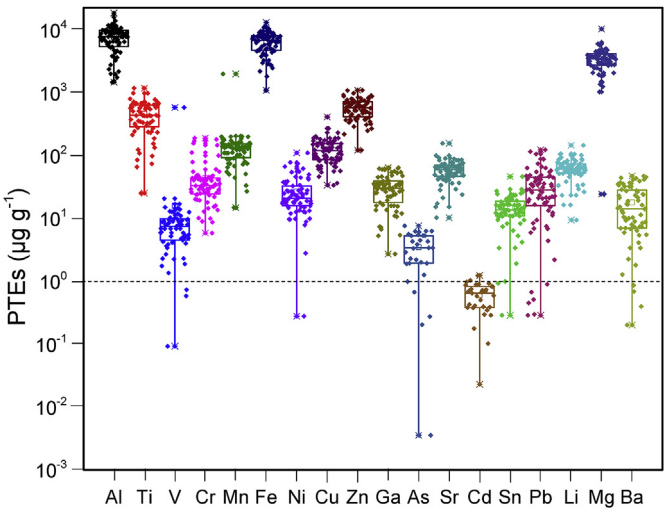

Fig. 2. Box plot showing concentration of PTEs (μg g^{-1}) in air conditioner dust, representing the overall enrichment of metals in indoor environment.

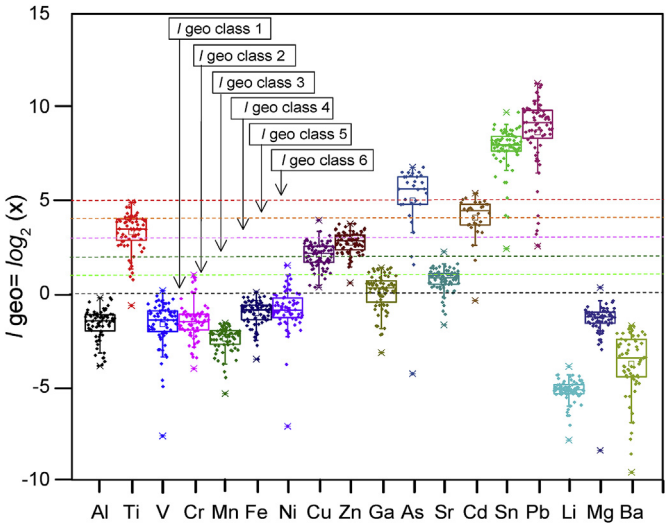

Fig. 3. Geo-accumulation index (I_{geo}) for various metal/metalloids identified in air conditioner dust from metropolitan area of Hefei, China.

Ga and Sr the values were >0 but <1 which indicates that these elements fall in a 2nd enrichment class. Cu and Zn were ranked as moderately to heavily contaminated as the I_{geo} values fall in 4th enrichment class (≤3). As and Cd were categorized as heavily to extremely contaminated as the I_{geo} value for these elements were ≤5 which indicates a high pollution status. The highest level of pollution was found in the case of Pb with an I_{geo} value of 8.63 followed by Sn with a value of 7.76. Household dust generation may be an important source of PTEs associated with both indoor and outdoor pollution sources (Ibanez et al., 2010). They can enter indoor environment either through the wind or with feet and some are generated within the indoor environment (Turner and Ip, 2007). Many PTEs including As, Zn, Pb, Cd and Sn were high in indoor environment as compared to outdoor (Olujimi et al., 2015). A study conducted in inner magnolia also revealed elevated bioaccumulation of Cd, Pb and As in dust and were categorized as 5th enrichment class (heavily polluted to extremely polluted) (Kexin et al., 2015). The high accumulation of Pb and Sn can be attributed to use of lead base paints, metallurgical products, heating and cooking activities and use of stainless steel utensils other than that vehicular emission play a key role in Pb emission which can infiltrate the indoor environment (Dundar and Altundag, 2002). The results of this study did not match with our previous study Ali et al., 2017a in which geo-accumulation of trace elements in road dust was found. This is possibly due to the reason that majority of particles form AC dust lies in the ultrafine NPs range and can carry PTEs due to its fine size and the large surface area which helps it to suspend in the air for a longer period. The reason may be the particles size as most of the particles identified in AC dust were in ultra-fine NPs range (Fig. 4) which can carry a lot of PTEs due to its small size and large surface area and remain suspended in the air for long period.

3.2. Cluster analysis and principle component analysis

Hierarchical cluster analysis was used to find out the linkage between PTEs found in AC dust. The results are illustrated in dendrogram Fig. S2. The first cluster appeared was in case of primary pair As-Cd while the second cluster was comprised of Ni-Ba-BC-Cr. A slightly weak cluster was found in case of Sn-Ga and Mg-Sr. A slightly strong cluster was observed in case of Pb-Zn-Fe while the

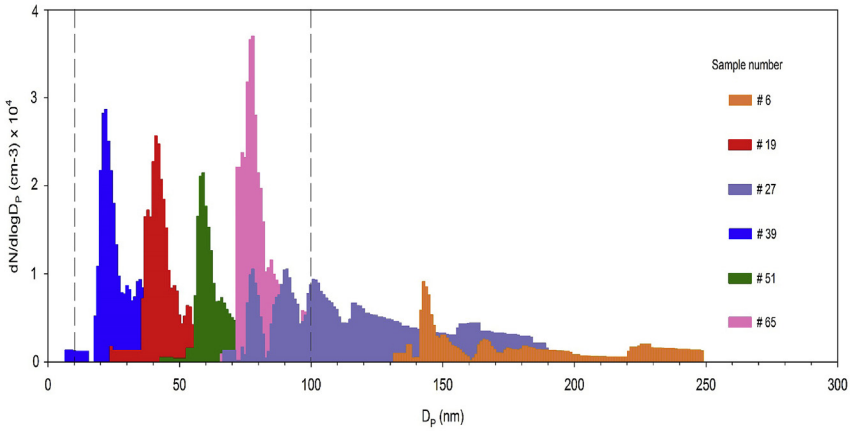

Fig. 4. Particles size distribution of air conditioner dust showing (a) no primary peak at (<10 nm) range (b) five primary peaks dominating in the ultra-fine nanoparticles region (<100 nm) (c) a 6th enrichment peak (>100 nm) at 145 nm.

strongest was found in case of Ti-Al. PCA was used in order to demonstrate the quantitative information about these cluster along with their corresponding sources. Two principle components (PCs) were employed with a total cumulative variance of 70.34% and eigen values of >1 illustrated in Fig. S3. The first quadrant of PC-I was dominated by elements like Al, Mn, Pb and V while the second quadrant was dominated by elements like Cu, Ti, Mg, Zn, Cr and Fe with a total variance of 37.78%. Most of these trace elements are originated as a result of industrial and vehicular emissions along with some indoor sources contribution such as electrical appliances, metallurgical products, heating and burning activates (Nazir et al., 2011), while Fe and Mn are mostly originated from steel and automobile manufacturing industries (Yang et al., 2016), which are found in Hefei and windblown soil/earth crust (Quiterioa et al., 2004). Cu is mostly used as a raw material while Zn is released as a result of brake wear emissions (Niu et al., 2010). In case of PC-II, the first quadrant was dominated by Ba, BC along with Ni and Sr with a total variance of 32.56%. Ba is mostly originated as a result of Vehicular brake wear (Yang et al., 2016), while BC as result of incomplete combustion of diesel and other organic products (Liu et al., 2011). The second quadrant of PC-II was dominated by Cd and As. In this case, Cd mostly originate as a result of burning fossil fuel while As can be attributed to mix sources as it is used in various industries (Nazir et al., 2011).

3.3. Particle size distribution

The particles size distribution pattern in AC dust observed in 6 samples is given in (Fig. 4). Among the studied samples five showed a major accumulation peak in ultrafine (<100 nm) except for 1 sample (6) for which the major accumulation peak was at 145 nm. The major accumulation peaks for the rest of the 5 samples were at 22 nm (sample 39), 40 nm (sample 19), 60 nm (sample 51), 78 nm (sample 65) and 91 nm (sample 27) but no particle peak was found in >10 nm range. The results of particles size distribution presented in this study did not matched with those reported by Yang et al. (2016). According to their results the primary peak was at 34 ± 1 nm, secondary peak was at 914 ± 46 nm and the rest were in 200–400 nm and 1000 nm but no peaks at ultra-fine range but in our case the distribution was dominated by ultra-fine NPs (<0.1 μm or 100 nm in diameter) as all of the peak accumulation in this study were in 22–100 nm range except for one sample having a peak at 145 nm. Our results are almost similar to those presented by Tiwari et al. (2013). According to them most of the primary accumulation peaks were in range 40–90 nm range and the average particles size was 40 nm, 65 nm and 90 nm which are comparable to the results documented in present article with an average particles size of 22 nm, 40 nm, 60 nm, 78 nm and 91 nm.

3.4. Dominant nanoparticles in AC dust

Based on the results of ICP-MS analysis samples 15 and 16 were selected based on their high metal concentration. These samples were analyzed using SEM along with EDS and TEM with SAED mode. The dominant NPs constitute of Pb, Cu, BC and Fe in addition to silica which is basically the main constituent of dust. The elemental mapping of dominant NPs in Ac dust is shown in (Fig. 5).

3.4.1. Lead nanoparticles

Pb Nano Particles identified using SEM/TEM are shown in (Fig. 6 b-C). The Pb NPs appear to be brighter in contrast as compared to other elements. The d spacing 0.28573 and 0.17498 revealed planes which were almost identical to (111) and (220) lattice fringes (Fig. S4) and appeared to be crystalline in nature having a size of 8–10 nm. The morphological structures appeared to be spherical but in some cases, rod-like structures were found. The results of TEM/EDS showed a strong relationship between Pb and other NPs like Sn, Pt, Zn, Ga and S whereas the association of Pb with Sn was found to be most dominant among these samples. The TEM/EDS/SAED revealed a dominant relationship between Pb particles and SnSo4 particles (Fig. 6 J1-J2). The results also indicate the existences of Lead sulfide (PbS) particles along with Zinc sulfide. The increased pollution level of Pb NPS is result of its special properties like its soft nature, highly ductility, corrosion resistance and low melting point and because of these properties it is being used worldwide in different industries like vehicles, paints, varnishes, plastic industries, ceramics industries etc. (Flora et al., 2012). PbS is widely used in PVC (polyvinyl chloride) pipes, cables and wires as a stabilizer whereas Pb and Sn solders are being used worldwide in electrical appliances (Arvidsson and Sanden, 2017). The relationship between Sb (antimony) and Pb NPs was also investigated in the AC dust. Sb is widely used in batteries alloys and also as a tracer in brake wear (Schauer et al., 2006).

3.4.2. Copper nanoparticles

Cu NPs found in AC dust using SEM/TEM are shown in (Fig. 6-D). The d-spacing 0.2073 and 0.1274 nm results revealed structures which were identical to that of cuprous oxide lattice planes (111) and (222) (Fig. S4). The TEM/EDS results show that the Cu NPs were well dispersed having a spherical morphological structure with the

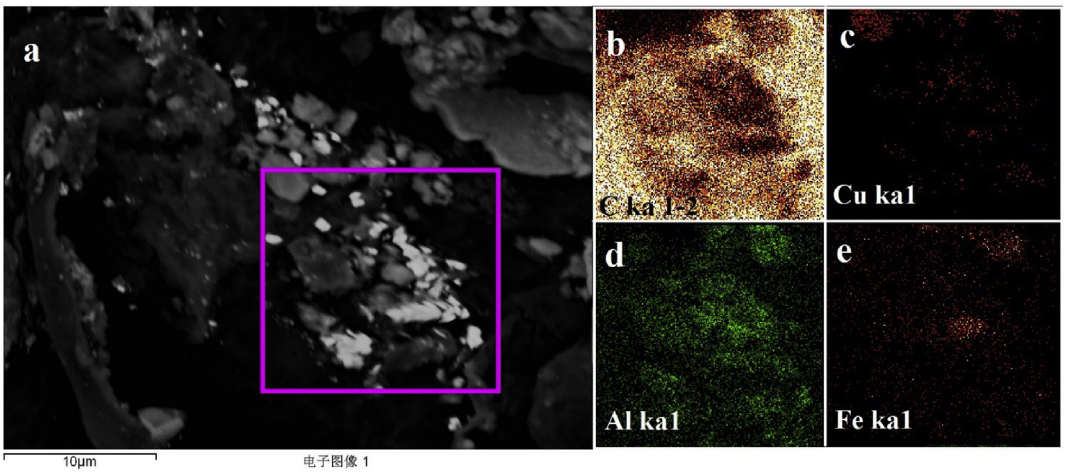

Fig. 5. TEM/EDS Elemental mapping of air conditioner dust: (a) Showing the selected area with aggregated nanoparticles; (b–e) showing the elemental map of carbon, Cu, Al and Fe in the selected area.

primary size of 5–15 nm range and a few nm width. TEM images of Cu NPs showed a Scherrer ring structure which indicates that these NPs were noncrystalline in nature. The dominant association of Cu was found to be with Al and Fe followed by sulfide, carbonates and Manganese oxides. In indoor environment, the presence of Cu particles was believed to be associated with the use of electrical appliances especially those used for cooling purpose (Nazir et al., 2011), and heating purpose (Wojdyga et al., 2014). Cu also contributes as an essential in brake wear and According to a study, more than 50–70% of the Cu release in Europe was associated with brake wear (Thorpe and Harrison, 2008). Due to high electrical conductivity and good optical properties, it is used worldwide in industries such as rubber industry, smelter, industries, power stations and fuel cells which in turn have increased the burden of Cu NPs in the atmosphere (Wang et al., 2015).

3.4.3. Iron nanoparticles

The iron oxides identified using SEM/TEM analysis are shown in (Fig. 6E–F) depicting a clear spherical shaped. These oxides are composed of Fe_2O_3 (hematite), Fe_3O_4 (magnetite), FeO (OH) (goethite). A d-spacing 0.48, 0.296 and 0.25 nm revealed lattice fringes which were similar to (111), (220) and (311) lattice planes of magnetite family (Fig. S4). The TEM results show Fe NPs to be in a strong relationship with particles like Sm, Ni, Al, Zn, Cr, Ga and Cu. The TEM/EDS image showed in obvious spherical shapes of magnetite particle which were surrounded by small size spherules (20–80 nm) and was found to be in combination with Pb, Cu, Pt, Sr, Zn and Mg. As compared to Fe_3O_4 aggregate the Fe_2O_3 were identified to be of very small particle size up to 15 nm Fe_2O_3 planes (110), (104), (113) were matched with d-spacing of 0.253, 0.271 and 0.221 nm. The results also revealed a strong association between BC and Fe oxides and in most cases, the relationship was found to be with Fe_2O_3. The primary source of Fe is believed to be originated naturally in dust from dry lands (Elzinga et al., 2011), but recent studies showed that the origin can also be associated with anthropogenic activities that release a significant amount of Fe into the atmosphere through combustion (Sedwick et al., 2007). It is released through vehicular emissions, braking system wear and tear and also decay of automobile frame and engine (Świetlik et al., 2015). In brake lining and brake disk iron oxides are used as abrasives which are degraded with application of brake (Chan and Stachowiak, 2004). Fly ash released from coal and vehicle exhaust emission often act is a source of magnetite NPs (Silva and Da Boit, 2011). Iron oxides are well-known regulator and stabilizers of organic carbon (Adhikari and Yang, 2015). Previous studies revealed that more than 20% of the organic carbon in dust was associated reactive iron oxides (Kaiser and Guggenberger, 2000).

3.4.4. Other nanoparticles

Other NPs identified using SEM/TEM/EDS are shown in supplementary information (Fig. S5, S6, S7, S8, S9, S10). Calcium (Ca) NPs were found in high concentration whereas calcium carbonate ($CaCO_3$) being most dominant in nature. The minerals like silica, calcium, quartz and clay are basically of natural origin which are released into the environment due to weathering process (Paltinean et al., 2016). Zinc oxides (ZnO) NPs in addition to zinc sulfide (ZnS) were also identified in SEM/TEM along with EDS images and the sources of origin for these NPs might be the vehicular emissions as the engineered NPs of ZnO are widely used in tires (Bystrzejewska-Piotrowska et al., 2009). The presence of amorphous silica can be attributed to its use in a variety of products such as tooth pastes, silicon rubbers, insulation, inks, cosmetics etc. (Merget et al., 2002). Platinum (Pt) and samarium (Sm) NPs were present in a minute amount with a diameter ranging from 1 to 10 nm. Pt is used in catalytic converters in order to reduce the pollution level of other elements like nitrogen oxides (NOx), Polycyclic Aromatic Hydrocarbons (PAHs) and carbon monoxides (CO) in vehicular emissions which lead to increased level of Pt NPs in the environment (Artelt and Levsen, 1999). TiO_2 NPs were also present in AC dust. These are widely used in paints to increase its durability, household and industrial products (paper mills, cutting oils, cosmetics etc.) (Kandavelu et al., 2004).

3.5. Black carbon

The mean value of BC was found to be 126 mg g^{-1}. The correlation results revealed a significant association ($R^2 = 0.78$) between BC and other PTEs (Fig. 7). The figure illustrates that the concentration of PTEs increased significantly with increase in concentration of BC. The results of SEM/TEM showed a high content of BC NPs in all the sample. The dark shaded areas mostly spherical in shape and grapes like clustered with size ranging from 40 to 120 nm (Fig. 6 (G-H-K1)) indicates the BC NPs. The BC NPs appeared to be in different shape which mainly depends on combustion mechanism. The dark black areas around the Fe NPs represents BC which indicated that Fe was trapped among a heavy fraction of BC clusters and

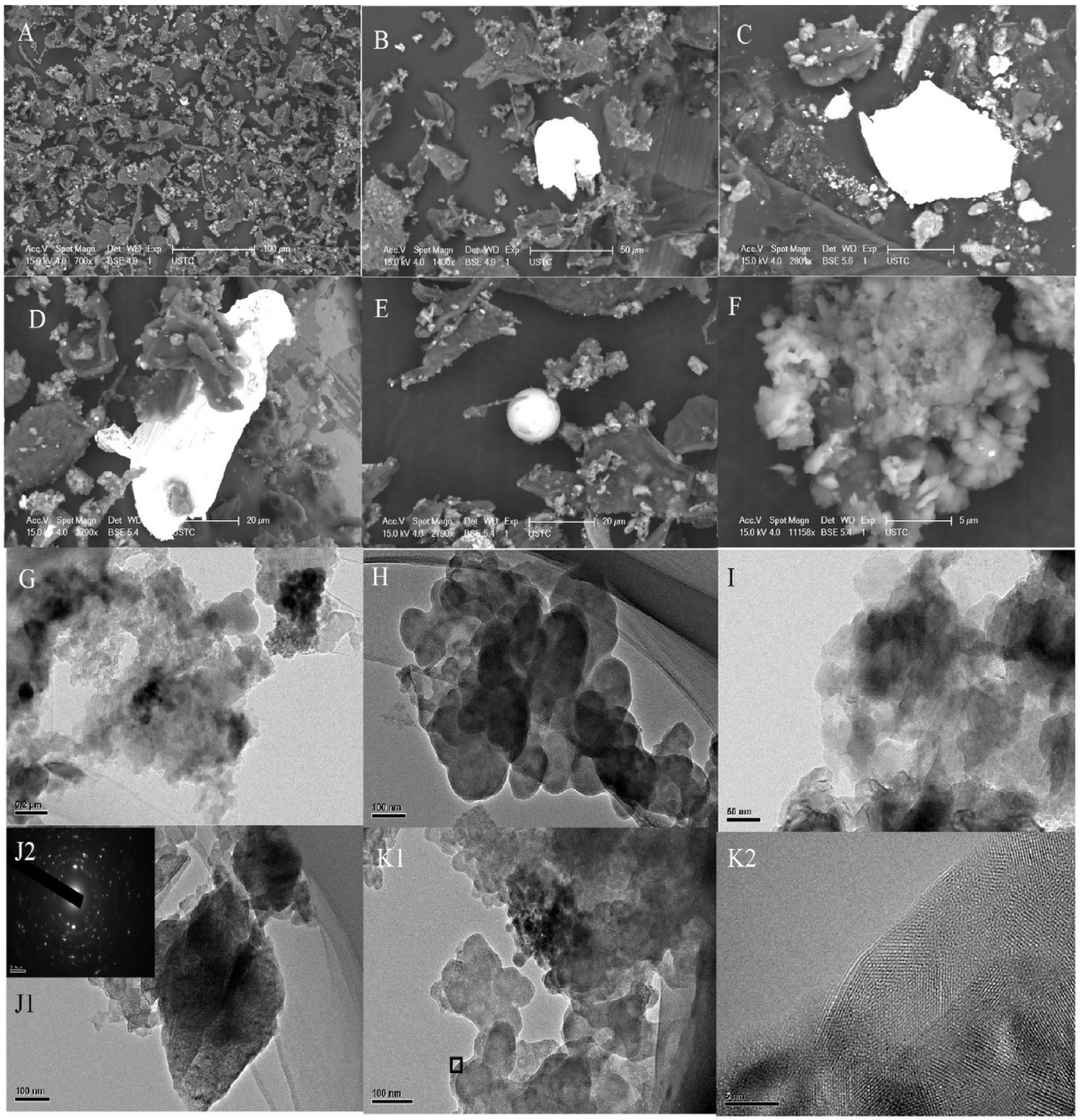

Fig. 6. SEM/TEM/EDS/SAED images showing various Fe, Cu, Pb and BC containing nanoparticles in air conditioner dust. A: SEM image showing distribution of dominant nanoparticles. B–C: SEM images showing typical Pb nanoparticles along with Cu particles in AC dust. D: SEM image showing a Cu rich nanoparticle. E–F: showing iron rich nanoparticle and crystalline structure in AC dust. G-H-I: TEM images showing association of Pb, Cu and Fe nano particles with black carbon. J1-J2: TEM along with SAED showing Pb rich particle association with $SnSO_4$. H1-2: TEM image showing an aggregate of Pb with $SnSO_4$ with primary size less than 50 nm and H2 shows the magnified selected area in H1.

these were concentrated along the sides of the Fe oxide NPs having non-homogeneous distribution throughout the whole complex and same was the case for Pb and Cu NPs. The SEM/TEM/EDS shows a significant association of dominant NPs (Pb, Cu, and Fe) with BC in AC dust. Other than these dominant NPs BC was found to be in strong association with Al, Mg, Ga, Sr, Sm, Pt, Au Cr. BC NPs remain suspended in the environments for several months due to its small size and have the ability travel a long distance before being deposited and their deposition is altered by various factors like source of emission (biomass and fossil fuel combustion, erosion of earth material), transport mode (air and water), weather conduction and distance from the emission sources (Zhan et al., 2016). Previous studies reveal that the high deposition of BC in the urban indoor environment is due to automobile exhaust emission (Han et al., 2011). The primary source for BC NPS includes types of emissions including smoking, combustion engines (Meng et al., 2017), printer emissions, cooking activities and dust resuspension in an indoor environment with poor ventilation (Isaxon et al., 2015). It can infiltrate the building through three main pathways (air and water), natural and mechanical ventilation and infiltration (Leung, 2015). Previous studies investigates that vehicular emissions impacts on indoor particulate and suggested that more than 70% of BC and 73% $PM_{0.1}$ particles in indoor environments are originated from the outdoor environment (Viana et al., 2011). In the case of indoor sources printing and photocopying contribute 20–25% and 15–20% by dust resuspension by residents and worker (Song et al., 2016). The PTEs concentration (Cd, Mn, Pb, V, Cu, Se, Zn, Sn, Sb, Mo, Ba) and BC concentration increase with decrease of

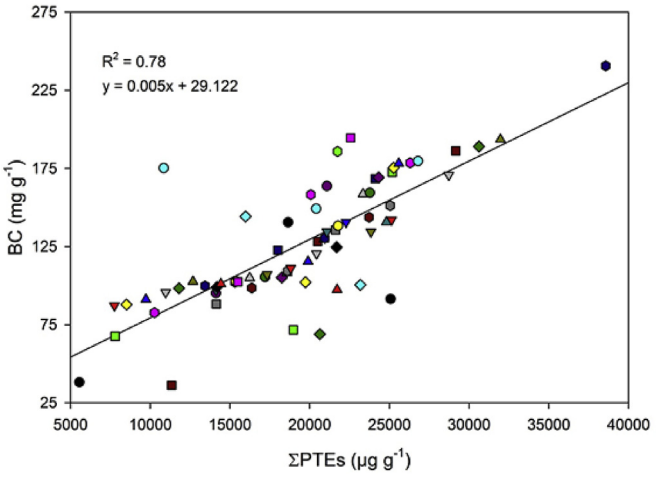

Fig. 7. Relationship between black carbon and potential toxic elements in air conditioner dust from metropolitan area of Hefei, China.

particles. BC often acts as a carriers for different types of toxins including trace elements, PAH and it also readily adsorbs gas particles due to its large surface area and small size, the trace elements concentration increase with an increase in the BC concentration (Isaxon et al., 2015).

4. Conclusion

Air-conditioner filters the air in order to provide a better air quality and during the filtration, most of the particles that get accumulated on the filters are ultra-fine particles due to its long-term suspension in air as compared to coarse particles which intend to settle down quickly which can provide good knowledge with respect to urban health, environmental hazards in our indoor environment and resident's exposure to these harmful hazards. Black carbon and nanoparticles in air-conditioner (AC) dust are important constituents of indoor air-pollution and is considered to be one of the top five environmental hazards. Nanoparticles, due to its small size, can pose a severe health risk as it has the ability to penetrate deep into the respiratory system. It is generated by re-suspension of dust from a variety of source including both anthropogenic and natural sources. In addition, black carbon acts as carrier for various PTEs and both have a strong positive correlation (0.78) indicating that the PTEs concentration increase with increase in BC content. Proper knowledge of these NPs and the PTEs attached to them can provide a better understanding in order to improve our indoor quality.

Acknowledgement

The authors greatly acknowledged the National Basic Research Program of China (973 Program, 2014CB238903), the National Natural Science Foundation of China (41672144 and **41402133**). The Chinese Academy of Science, China (CAS) and The World Academy of Science, Italy (TWAS) are also greatly acknowledged for providing the CAS-TWAS President's fellowship (CAS-TWAS No. 2014-179). We also greatly appreciate the thoughtful comments and valuable suggestions from anonymous reviewers for the improvement of this manuscript.

Appendix A. Supplementary data

Supplementary data related to this article can be found at https://doi.org/10.1016/j.jclepro.2018.01.161.

References

Adhikari, D., Yang, Y., 2015. Selective stabilization of aliphatic organic carbon by iron oxide. Sci. Rep. 5, 11214. https://doi.org/10.1038/srep11214.
Ali, M.U., Liu, G., Yousuf, B., Abbas, Q., Munir, M.A.M., Fu, B., 2017a. Pollution characteristics and human health risks of potentially (eco) toxic element (PTEs) in road dust from metropolitan area of Hefei, China. Chemosphere 181, 111–121. https://doi.org/10.1016/j.chemosphere.2017.04.061.
Ali, M.U., Rashid, A., Yousuf, B., Kamal, A., 2017b. Health outcomes of road-traffic pollution among exposed roadside-workers in the Rawalpindi City Pakistan. Hum. Ecol. Risk Assess. An Int. J. 7039 https://doi.org/10.1080/10807039.2017.1308814, 00–00.
Artelt, S., Levsen, K., 1999. Bioavailability of finely dispersed platinum as emitted from automotive catalytic converter: a model study. Sci. Total Environ. 228, 217–226.
Arvidsson, R., Sanden, B.A., 2017. Carbon nanomaterials as potential substitutes for scarce metals. J. Clean. Prod. J. 156, 253–261. https://doi.org/10.1016/j.jclepro.2017.04.048.
Bekö, G., Halás, O., Clausen, G., Weschler, C.J., 2006. Initial studies of oxidation processes on filter surfaces and their impact on perceived air quality. Indoor Air 16, 56–64. https://doi.org/10.1111/j.1600-0668.2005.00401.x.
Bystrzejewska-Piotrowska, G., Golimowski, J., Urban, P.L., 2009. Nanoparticles: their potential toxicity, waste and environmental management. Waste Manag. 29, 2587–2595. https://doi.org/10.1016/j.wasman.2009.04.001.
Cempel, M., Nikel, G., 2006. Nickel: a review of its sources and environmental toxicology. Pol. J. Environ. Stud. 15, 375–382. https://doi.org/10.1109/TUFFC.2008.827.
Chan, D., Stachowiak, G.W., 2004. Review of automotive brake friction materials. Proc. Inst. Mech. Eng. - Part D J. Automob. Eng. 218, 953–966. https://doi.org/10.1243/0954407041856773.
Chen, X., Xia, X., Zhao, Y., Zhang, P., 2010. Heavy metal concentrations in roadside soils and correlation with urban traffic in Beijing, China. J. Hazard Mater. 181, 640–646. https://doi.org/10.1016/j.jhazmat.2010.05.060.
Dundar, M.S., Altundag, H., 2002. Heavy metal determinations of house dusts in Adapazari city, Turkey after earthquake. Trace Elem. Electrolytes 19, 55–58.
Elzinga, E.J., Gao, Y., Fitts, J.P., Tappero, R., 2011. Iron speciation in urban dust. Atmos. Environ. 45, 4528–4532. https://doi.org/10.1016/j.atmosenv.2011.05.042.
Flora, G., Gupta, D., Tiwari, A., 2012. Toxicity of lead: a review with recent updates. Interdiscipl. Toxicol. 5, 47–58. https://doi.org/10.2478/v10102-012-0009-2.
Glaser, B., Dreyer, A., Bock, M., Fiedler, S., Mehring, M., Heitmann, T., 2005. Source apportionment of organic pollutants of a highway-traffic-influenced urban area in Bayreuth (Germany) using biomarker and stable carbon isotope signatures. Environ. Sci. Technol. 39, 3911–3917. https://doi.org/10.1021/es050002p.
Gramotnev, G., Ristovski, Z., 2004. Experimental investigation of ultra-fine particle size distribution near a busy road. Atmos. Environ. 38, 1767–1776. https://doi.org/10.1016/j.atmosenv.2003.12.028.
Gramsch, E., Reyes, F., Oyola, P., Rubio, M. a., López, G., Pérez, P., Martínez, R., 2014. Particle size distribution and its relationship to black carbon in two urban and one rural site in Santiago de Chile. J. Air Waste Manag. Assoc. 64, 785–796. https://doi.org/10.1080/10962247.2014.890141.
Graudenz, G.S., Oliveira, C.H., Tribess, A., Mendes, C., Latorre, M.R.D.O., Kalil, J., 2005. Association of air-conditioning with respiratory symptoms in office workers in tropical climate. Indoor Air 15, 62–66. https://doi.org/10.1111/j.1600-0668.2004.00324.x.
Han, Y.M., Cao, J.J., Yan, B.Z., Kenna, T.C., Jin, Z.D., Cheng, Y., Chow, J.C., An, Z.S., 2011. Comparison of elemental carbon in lake sediments measured by three different methods and 150-year pollution history in eastern China. Environ. Sci. Technol. 45, 5287–5293. https://doi.org/10.1021/es103518c.
Hussein, T., Glytsos, T., Ondráček, J., Dohányosová, P., Ždímal, V., Hämeri, K., Lazaridis, M., Smolík, J., Kulmala, M., 2006. Particle size characterization and emission rates during indoor activities in a house. Atmos. Environ. 40, 4285–4307. https://doi.org/10.1016/j.atmosenv.2006.03.053.
Ibanez, Y., Le Bot, B., Glorennec, P., 2010. House-dust metal content and bioaccessibility: a review. Eur. J. Mineral 22, 629–637. https://doi.org/10.1127/0935-1221/2010/0022-2010.
Isaxon, C., Gudmundsson, A., Nordin, E.Z., Lonnblad, L., Dahl, A., Wieslander, G., Bohgard, M., Wierzbicka, A., 2015. Contribution of indoor-generated particles to residential exposure. Atmos. Environ. 106, 458–466. https://doi.org/10.1016/j.atmosenv.2014.07.053.
Johnson, K.S., Zuberi, B., Molina, L.T., Molina, M.J., Iedema, M.J., Cowin, J.P., Gaspar, D.J., Wang, C., 2005. Processing of soot in an urban environment : case study from the Mexico City Metropolitan Area. Atmos. Chem. Phys. 4, 3033–3043.
Kaiser, K., Guggenberger, G., 2000. The role of DOM sorption to mineral surfaces in the preservation of organic matter in soils, 31, 711–725.
Kandavelu, V., Kastien, H., Ravindranathan Thampi, K., 2004. Photocatalytic degradation of isothiazolin-3-ones in water and emulsion paints containing nanocrystalline TiO2 and ZnO catalysts. Appl. Catal. B Environ. 48, 101–111. https://doi.org/10.1016/j.apcatb.2003.09.022.
Kexin, L., Liang, T., Wang, L., Yang, Z., 2015. Contamination and health risk assessment of heavy metals in road dust in Bayan Obo Mining Region in Inner Mongolia, North China. J. Geogr. Sci. 25, 1439–1451. https://doi.org/10.1007/

s11442-015-1244-1.
Leung, D.Y.C., 2015. Outdoor-indoor air pollution in urban environment: challenges and opportunity. Front. Environ. Sci. 2, 1–7. https://doi.org/10.3389/fenvs.2014.00069.
Lighty, J.S., Veranth, J.M., Sarofim, A.F., 2000. Combustion aerosols: factors governing their size and composition and implications to human health. J. Air Waste Manag. Assoc. 50 https://doi.org/10.1080/10473289.2000.10464197, 1565–1618-1622.
Liu, S., Xia, X., Zhai, Y., Wang, R., Liu, T., Zhang, S., 2011. Black carbon (BC) in urban and surrounding rural soils of Beijing, China: spatial distribution and relationship with polycyclic aromatic hydrocarbons (PAHs). Chemosphere 82, 223–228. https://doi.org/10.1016/j.chemosphere.2010.10.017.
Meng, J., Mi, Z., Yang, H., Shan, Y., Guan, D., Liu, J., 2017. The consumption-based black carbon emissions of China's megacities. J. Clean. Prod. 161, 1275–1282. https://doi.org/10.1016/j.jclepro.2017.02.185.
Merget, R., Bauer, T., Küpper, H.U., Philippou, S., Bauer, H.D., Breitstadt, R., Bruening, T., 2002. Health hazards due to the inhalation of amorphous silica. Arch. Toxicol. 75, 625–634. https://doi.org/10.1007/s002040100266.
Müller, G., 1979. Schwermetalle in den sedimenten des Rheins-Veranderungenseit. Umsch Wiss Tech, pp. 778–783.
Nazir, R., Shaheen, N., Shah, M.H., 2011. Indoor/outdoor relationship of trace metals in the atmospheric particulate matter of an industrial area. Atmos. Res. 101, 765–772. https://doi.org/10.1016/j.atmosres.2011.05.003.
Niu, J., Rasmussen, P.E., Hassan, N.M., Vincent, R., 2010. Concentration distribution and bioaccessibility of trace elements in nano and fine urban airborne particulate matter: influence of particle size. Water, Air, Soil Pollut. 213, 211–225. https://doi.org/10.1007/s11270-010-0379-z.
Olujimi, O., Steiner, O., Goessler, W., 2015. Pollution indexing and health risk assessments of trace elements in indoor dusts from classrooms, living rooms and offices in Ogun State, Nigeria. J. Afr. Earth Sci. 101, 396–404. https://doi.org/10.1016/j.jafrearsci.2014.10.007.
Paltinean, A.G., Petean, I., Arghir, G., Florina, D., Bobos, L., Tomoaia-cotisel, M., Gertrud, A., Petean, I., Arghir, G., Muntean, F., Bobos, L., Tomoaia-cotisel, M., 2016. Atmospheric induced nanoparticles due to the urban street dust. Part. Sci. Technol. 34, 580–585. https://doi.org/10.1080/02726351.2015.1090509.
Patel, M., Azanza Ricardo, C.L., Scardi, P., Aswath, P.B., 2012. Morphology, structure and chemistry of extracted diesel soot—Part I: Transmission electron microscopy, Raman spectroscopy, X-ray photoelectron spectroscopy and synchrotron X-ray diffraction study. Tribol. Int. 52, 29–39. https://doi.org/10.1016/j.triboint.2012.03.004.
Quiterioa, S.L., da Silvaa, R.S., Arbillaa, G., Escaleirab, V., 2004. Metals in airborne particulate matter in the industrial district of Santa Cruz, Rio de Janeiro, in an annual period Simone. AE Int. Cent. South Am. 38, 321–331. https://doi.org/10.1016/j.atmosenv.2003.09.017.
Sahu, D., Kannan, G.M., Vijayaraghavan, R., 2014. Carbon black particle exhibits size dependent toxicity in human monocytes. Int. J. Inflamm. 2014 https://doi.org/10.1155/2014/827019.
Schauer, J.J., Lough, G.C., Shafer, M.M., Christensen, W.F., Arndt, M.F., DeMinter, J.T., Park, J.S., 2006. Characterization of metals emitted from motor vehicles. Res. Rep. Health Eff. Inst. 1, 76–88.
Sedwick, P.N., Sholkovitz, E.R., Church, T.M., 2007. Impact of anthropogenic combustion emissions on the fractional solubility of aerosol iron: evidence from the Sargasso Sea. Geochem. Geophys. Geosyst. 8, 1–21. https://doi.org/10.1029/2007GC001586.
See, S.W., Karthikeyana, S., Balasubramanian, R., 2006. Health risk assessment of occupational exposure to particulate-phase polycyclic aromatic hydrocarbons associated with Chinese, Malay and Indian cooking. J. Environ. Monit. 8, 369–376. https://doi.org/10.1039/b516173h.
Silva, L.F.O., Da Boit, K.M., 2011. Nanominerals and nanoparticles in feed coal and bottom ash: implications for human health effects. Environ. Monit. Assess. 174, 187–197. https://doi.org/10.1007/s10661-010-1449-9.
Song, X., Hao, Y., Zhang, C., Peng, J., Zhu, X., 2016. Vehicular emission trends in the Pan-Yangtze river delta in China between 1999 and 2013. J. Clean. Prod. 137, 1045–1054. https://doi.org/10.1016/j.jclepro.2016.07.197.
Świetlik, R., Trojanowska, M., Strzelecka, M., Bocho-Janiszewska, A., 2015. Fractionation and mobility of Cu, Fe, Mn, Pb and Zn in the road dust retained on noise barriers along expressway - a potential tool for determining the effects of driving conditions on speciation of emitted particulate metals. Environ. Pollut. 196, 404–413. https://doi.org/10.1016/j.envpol.2014.10.018.
Thorpe, A., Harrison, R.M., 2008. Sources and properties of non-exhaust particulate matter from road traffic : a review. Sci. Total Environ. 400, 270–282. https://doi.org/10.1016/j.scitotenv.2008.06.007.
Tiwari, A.J., Fields, C.G., Marr, L.C., 2013. A cost-effective method of aerosolizing dry powdered nanoparticles. Aerosol. Sci. Technol. 47, 1267–1275. https://doi.org/10.1080/02786826.2013.834292.
Turner, A., Ip, K.H., 2007. Bioaccessibility of metals in dust from the indoor environment: application of a physiologically based extraction test. Environ. Sci. Technol. 41, 7851–7856. https://doi.org/10.1021/es071194m.
Ullah, H., Liu, G., Yousaf, B., Ubaid, M., Abbas, Q., 2017. Combustion characteristics and retention-emission of selenium during co- fi ring of torre fi ed biomass and its blends with high ash coal. Bioresour. Technol. 245, 73–80. https://doi.org/10.1016/j.biortech.2017.08.144.
Verdenelli, M.C., Cecchini, C., Orpianesi, C., Dadea, G.M., Cresci, A., 2003. Efficacy of antimicrobial filter treatments on microbial colonization of air panel filters. J. Appl. Microbiol. 94, 9–15. https://doi.org/10.1046/j.1365-2672.2003.01820.x.
Viana, M., Díez, S., Reche, C., 2011. Indoor and outdoor sources and in filtration processes of PM 1 and black carbon in an urban environment. Atmos. Environ. 45, 6359–6367. https://doi.org/10.1016/j.atmosenv.2011.08.044.
Wan, M.P., Wu, C.L., Sze To, G.N., Chan, T.C., Chao, C.Y.H., 2011. Ultrafine particles, and PM2.5 generated from cooking in homes. Atmos. Environ. 45, 6141–6148. https://doi.org/10.1016/j.atmosenv.2011.08.036.
Wang, L.F., Habibul, N., He, D.Q., Li, W.W., Zhang, X., Jiang, H., Yu, H.Q., 2015. Copper release from copper nanoparticles in the presence of natural organic matter. Water Res. 68, 12–23. https://doi.org/10.1016/j.watres.2014.09.031.
Wojdyga, K., Chorzelski, M., Rozycka-wronska, E., 2014. Emission of pollutants in fl ue gases from Polish district heating sources. J. Clean. Prod. 75, 157–165. https://doi.org/10.1016/j.jclepro.2014.03.069.
Yang, Y., Vance, M., Tou, F., Tiwari, A., Liu, M., Hochella, M.F., 2016. Nanoparticles in road dust from impervious urban surfaces: distribution, identification, and environmental implications. Environ. Sci. Nano 3, 534–544. https://doi.org/10.1039/C6EN00056H.
Yinon, L., Themelis, N.J., McNeill, V.F., 2010. Ultrafine particles from WTE and other combustion sources. In: 18th Annu. North Am. Waste-to-Energy Conf, vol. 7, pp. 1–16. https://doi.org/10.1115/NAWTEC18-3581.
Yousaf, B., Liu, G., Abbas, Q., Wang, R., Ubaid, M., Ullah, H., Liu, R., Zhou, C., 2017. Systematic investigation on combustion characteristics and emission- reduction mechanism of potentially toxic elements in biomass- and biochar- coal co-combustion systems. Appl. Energy 208, 142–157. https://doi.org/10.1016/j.apenergy.2017.10.059.
Yousaf, B., Liu, G., Wang, R., Zia-ur-Rehman, M., Rizwan, M.S., Imtiaz, M., Murtaza, G., Shakoor, A., 2016. Investigating the potential influence of biochar and traditional organic amendments on the bioavailability and transfer of Cd in the soil–plant system. Environ. Earth Sci. 75, 1–10. https://doi.org/10.1007/s12665-016-5285-2.
Yu, B.F., Hu, Z.B., Liu, M., Yang, H.L., Kong, Q.X., Liu, Y.H., 2009. Review of research on air-conditioning systems and indoor air quality control for human health. Int. J. Refrig. 32, 3–20. https://doi.org/10.1016/j.ijrefrig.2008.05.004.
Zhan, C., Zhang, J., Cao, J., Han, Y., Wang, P., Zheng, J., Yao, R., Liu, H., Li, H., Xiao, W., 2016. Characteristics and sources of black carbon in atmospheric dustfall particles from huangshi, China. Aerosol Air Qual. Res. 16, 2096–2106. https://doi.org/10.4209/aaqr.2015.09.0562.
Zhang, R., Wang, H., Qian, Y., Rasch, P.J., Easter, R.C., Ma, P., Singh, B., Huang, J., Fu, Q., 2015. Quantifying sources, transport, deposition, and radiative forcing of black carbon over the Himalayas and Tibetan Plateau. Atmos. Chem. Phys. 15, 6205–6223. https://doi.org/10.5194/acp-15-6205-2015.